Agglomeration and uniform growth of Si_3N_4 on Si(100): Experiments and first-principles calculations

Koichi Kato,* Daisuke Matsushita, Koichi Muraoka, and Yasushi Nakasaki
Advanced LSI Technology Laboratory, Toshiba Corporate Research and Development Center, 1 Komukai Toshiba-cho, Saiwai-ku, Kawasaki 210-8582, Japan

(Received 15 February 2008; revised manuscript received 26 May 2008; published 26 August 2008)

We studied agglomeration and uniform growth of Si_3N_4 by condensation of N atoms incorporated in crystalline Si. Agglomeration of Si_3N_4 and atomically flat growth of highly coordinated Si_3N_4 on Si(100) surfaces were observed distinguishably with appropriate temperature and growth rate conditions. Based on first-principles calculations, charge transfers between Si and N atoms were found to enhance electrostatic energy between them, leading to Si-N network organization in crystalline Si. Although rapid N introduction upon Si(100) surfaces brings about agglomeration of Si_3N_4 materials, gradual N incorporation is likely to form a stable SiN layer network around the third layer to serve as a seed layer for uniform thin Si_3N_4 film growth on Si(100) surfaces. When a Si_3N_4 film on Si(100) is closer to an ideal structure with smaller defects, it will grow thicker than normal nitridation with higher strain energy.

DOI: 10.1103/PhysRevB.78.085321 PACS number(s): 73.61.Ng, 61.66.−f

I. INTRODUCTION

With scaling down of metal-oxide-semiconductor field-effect transistors (MOSFETs) in Si large-scale integration (LSI) technology, thickness of gate insulating films has been approaching the scaling limit, where tunneling currents dominate device degradation and performance. High-*k* dielectric films, which are expected to reduce tunneling currents, are considered to be promising alternatives to SiO_2 films or N-incorporated SiO_2 films. Those materials have been widely and intensively studied. In these circumstances, atomically layered and perfectly coordinated Si_3N_4 films with slight SiO_2 at the interface, if those films can be successfully formed, would not only be moderately high-*k* dielectrics with minimum interfaces capable of substituting for SiO_2 films or N-incorporated SiO_2 films but also interface layers for high-*k* dielectrics.

Nitridation of Si surfaces and interfaces employs thermal reactions of N-containing gas molecules such as NH_3[1–3] or plasma-assisted N-atom radicals.[4] The chemical vapor deposition has been extensively employed for silicon nitride films with substantial thickness in actual devices. When we try to form thinner SiN_x films by incorporating NH_3 molecules or plasma-assisted N-atom radicals on Si surfaces, however, it becomes increasingly difficult to fabricate with an atomically flat or a uniform thickness structure. SiN_x films sometimes become discontinuous, and moreover, isolated into small volumes on Si surfaces with thickness of less than 1 nm.[5] This behavior may be characterized microscopically as self-condensation and agglomeration of silicon nitrides. Furthermore, thickness of Si nitridation cannot exceed a few nanometers in thickness. In contrast, oxidation of Si occurs with a layer-by-layer mode and this mode continues at SiO_2/Si interfaces even in the case of oxides with thickness of several nanometers.[6–8] Thickness of Si oxidation can be extended in so far as oxygen molecules migrate into SiO_2/Si interfaces. Those behaviors specific to Si nitridation are thought to reflect the nature of Si-N bond organization.

The aim of the present study is to understand the mechanisms of Si nitridation through N incorporation in Si substrates and to study growth modes of Si nitridation on Si(100) substrates, leading to atomically uniform thin Si nitride films on Si surfaces. We performed Si(100) nitridation by experimental techniques, where generated structures exhibit remarkable changes in accordance with experimental procedures. Then, we tried to elucidate the atomic mechanism of this Si nitridation through first-principles calculations. Finally, we investigated a uniform Si nitride without defects on Si(100) substrates and analyzed its atomic and electronic structures.

II. CALCULATION AND EXPERIMENTAL METHODS

A Si(100) substrate was boiled in H_2SO_4 and H_2O_2 solution, and then treated with 0.5% dilute HF solution before nitridation. Si nitridation was performed by exposing the clean Si(100) surface to NH_3 molecules.[9] The base pressure for nitridation of our sysytem is 0.01 Torr. It is increased up to 0.3 Torr for a growth rate of 0.01 nm/s, and up to 740 Torr for a growth rate of 0.1 nm/s. Then, we carried out atomic force microscope (AFM) experiments and x-ray photoelectron spectroscopy (XPS) observations. The thickness of Si nitride was measured by XPS and ellipsometry.

Our calculations are based on density-functional theory (DFT) and generalized gradient approximation (GGA) to describe nitrogen properties properly.[10] The calculations were performed using ultrasoft pseudopotentials[11] for nitrogen and oxygen atoms with 1 to 8 k points for Brillouin-zone samplings. We found that the cut-off energies of 25 Ry for the wave functions and 144 Ry for the augmented electron densities are sufficient for converging energies.[10] All the calculations were performed with a repeated supercell consisting of 64 Si atoms or a repeated slab modified from a $c(4\times4)$ surface unit cell, consisting of 14 layers of Si atoms and a vacuum spacing with the same thickness. Inversion symmetry with respect to the slab center located at a Si bond center is used for surfaces to increase the computational efficiency. An effective charge of valence electrons for each atom is evaluated by summing the charge densities within its

 ©2008 The American Physical Society

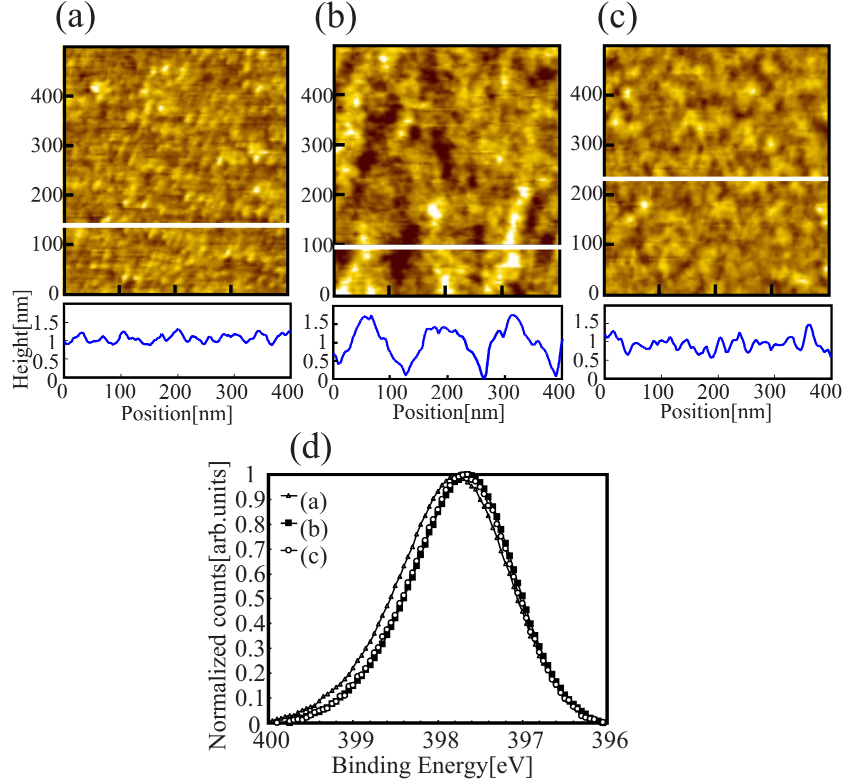

FIG. 1. (Color online) Top views and cross-sectional profiles of AFM observation for nitrided Si(100) surfaces grown (a) with 0.1 nm/s and at room temperature, (b) with 0.1 nm/s and at 850 °C, and (c) with 10^{-2} nm/s and at 850 °C. The cross-section is denoted with a line on the top views.(d) XPS observation of N 1s spectra for nitrided Si(100) surfaces for (a), (b), and (c) conditions.

Wigner-Seitz cell,[12] which can be calculated at grid points generated regularly on Cartesian coordinates. Practically, the charge density defined at each grid point belongs to the atom closest to the grid point.

III. RESULTS AND DISCUSSION

A. Nitridation processes on Si(100)

Among various temperature and growth rate conditions examined so far, we show representative nitridation processes on Si(100) surfaces. A Si nitride of 1.0 nm thickness was grown with a growth rate of 0.1 nm/s [Fig. 1(a)] at room temperature (RT) and [Fig. 1(b)] at appropriately chosen 850 °C. The surface morphology of Si nitrides for both cases was observed by AFM, as shown in Figs. 1(a) and 1(b), respectively. A large surface roughness is, however, noticed in the top view of nitrided Si(100) in Fig. 1(b). The large roughness oscillation with a period around 100 nm is obvious in the cross-sectional profile of Fig. 1(b), corresponding well to the previous reported observation.[5] Rapid N incorporation at high temperature thus resulted in agglomeration of Si nitrides and moreover, to discontinuous Si nitride films.

In the case of a Si nitride of 1.0 nm thickness grown with a slow growth rate of 0.01 nm/s at 850 °C, the surface roughness was surprisingly reduced as is clearly revealed by comparing the top view in Fig. 1(c) with Fig. 1(b). Large roughness oscillation also disappeared in the cross-sectional profile in Fig. 1(c), whereas it is present in Fig. 1(b), and atomically flatter growth of Si_3N_4 films was achieved by reducing the growth rate. The N 1s spectra for Figs. 1(b) and 1(c) observed by XPS shown in Fig. 1(d) suggest that $N\equiv Si_3$ species (the second nearest of N is N) is the majority component, because they agree well with the experiment[13] and the theory.[14] In contrast, higher energy components corresponding to $H-N=Si$ and $H_2=N-Si$ are enhanced in the case of Fig. 1(a).

B. N atom stable configurations

To understand N incorporation behaviors into crystalline Si, calculations were performed for N-atom-adsorbed Si crystals. Figure 2 shows calculated stable configurations for interstitial and substitutional N atoms in the crystalline Si with N adsorption energy and energy barriers between each configuration for 1 k point. Here, we express energy gains for N adsorption per N atom $E_{ad}(N)$ by

$$E_{ad}(N) = [E(Si_{cry}) + E(N_{atoms}) - E(Si_{atoms\text{-}cry}) - E(Si_{cry}\ \text{with}\ N)]/n_N, \quad (1)$$

where $E(Si_{cry})$, $E(N_{atoms})$, $E(Si_{atoms\text{-}cry})$, and $E(Si_{cry}$ with N) represent energies for a Si crystal, N atoms, Si atoms constituting a crystal Si, and an N-adsorbed Si crystal, respectively. n_N denotes the number of adsorbed N atoms. The Si atoms substituted by N atoms are assumed to move into a bulk Si site. For calculating transitions from Fig. 2(a) to Fig. 2(c) and Fig. 2(d), and from Fig. 2(d) to Fig. 2(e) the energy

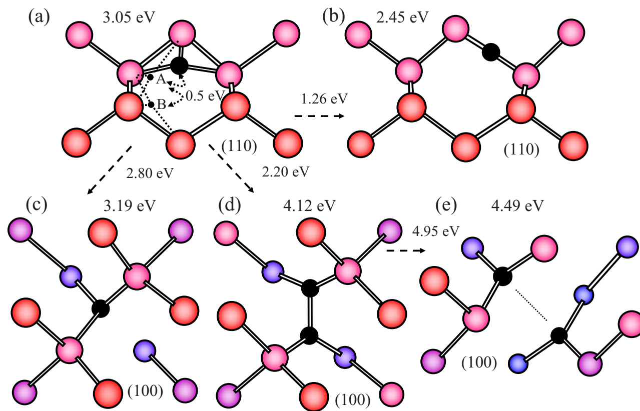

FIG. 2. (Color online) (a), (b), (c), (d), and (e) Stable configurations for interstitial and substitutional N atoms in crystalline Si with N adsorption energy and energy barriers from (a) to (b), (c) and (d), and from (d) to (e) configurations. Dark circles represent N atoms. Bright circles represent Si atoms from red to blue according to the depth.

required for interstitial Si generation is automatically included in energy barriers. The energy gain for an interstitial N atom is [Fig. 2(a)] 3.05 eV at a ⟨110⟩ split-interstitial configuration and [Fig. 2(b)] 2.45 eV at a Si bond center with a small difference from 3.38 and 2.83 eV for 8 k point samplings, respectively. The interstitial N migrates between equivalent threefold configurations with a small energy barrier of 0.5 eV, as represented by the broken curves to A and to B in Fig. 2(a).[15] The energy gain for N adsorption is increased up to [Fig. 2(c)] 3.19 eV at a substitutional site to [Fig. 2(d)] 4.12 eV/N atom at two split-interstitial sites, and furthermore to [Fig. 2(e)] 4.49 eV/N atom at neighboring substitutional sites, where no dangling bond (DB) is exposed. The values, which agree quite well with the previous reported values,[16,17] are surprisingly small compared to 6.93 eV calculated for N adsorption in α-Si_3N_4 and 7.16 eV for N adsorption in β-Si_3N_4.[18] In contrast, the energy gain of O adsorption does not differ greatly between O atoms in a Si crystal (5.0–6.7 eV) and in α-SiO_2 (7.3 eV).[8] Since the transition from Figs. 2(d) and 2(e) generates a Si interstitial, the large energy barrier of 4.95 eV is needed for this transition, indicating that the stable structure of nearest-neighbor Si substitution by two N atoms is not easy at low temperature.

C. N-atom cluster condensation

Although energy gain by adsorption of an N atom isolated in crystalline Si is small, condensation of N atoms in the crystalline Si generates large energy gain. Typical examples of N-condensed structures in the crystalline Si are shown in Fig. 3. Initially located at split-interstitial configurations, N atoms were relaxed to realize the most stable configurations. Although the energy gain by formation of an N-Si-N cluster in Fig. 3(a) is only 3.19 eV/N atom, that is, an increase of only 0.14 eV from Fig. 2(a), the energy gain is rapidly increased to 5.22 eV/N atom in Fig. 3(b), closer to the N adsorption energy in the crystalline Si_3N_4. The N adsorption energy in crystalline Si_3N_4 is evaluated as 7.03 eV for α-Si_3N_4, and 7.02 eV for β-Si_3N_4 from the reported experimental results.[19] The energy gain by condensation of three N atoms in Fig. 3(c) is 5.03 eV/N atom, being slightly decreased from Fig. 3(b). This value is further decreased to 4.20 eV/N atom in condensation of four N atoms in Fig. 3(d). The remarkable difference in the energy gain for each atomic configuration is associated with the number of nearest-neighbor N atoms per Si atom. Here, N atoms are defined as nearest neighbors to a Si atom, if the N atoms are one of the four nearest-neighbor atoms to the Si atom. To simply estimate chemical bonds between Si and N atoms, N atoms are assumed to have a bond with a Si atom when N atoms are nearest neighbors to the Si atom. Only one N-Si-N bond [N(1)-Si(1)-N(2)] is formed in Fig. 3(a), whereas two N-Si-N bonds [N(1)-Si(1)-N(2) and N(1)-Si(2)-N(2)] are formed in Fig. 3(b). The number of N-Si-N bonds/N atom

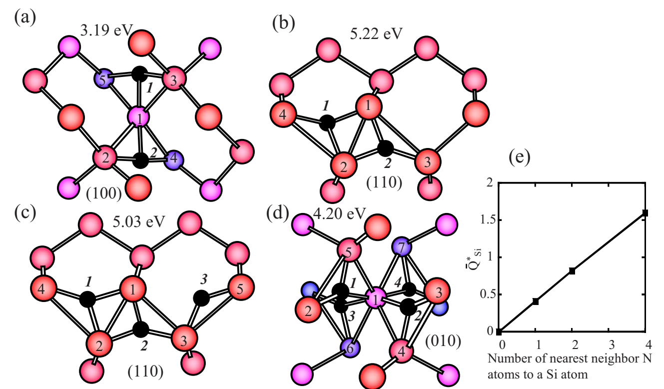

FIG. 3. (Color online) (a), (b), (c), and (d) N-condensed structures in crystalline Si with N adsorption energy. Adsorption energy/N atom increases in proportion to the number of N atoms adjacent to the same Si atom in (b), (c), and (d). Dark circles represent N atoms. Bright circles represent Si atoms from red to blue according to the depth. (e) The average effective charge on Si atoms ($\bar{Q}^*_{Si}$) with a unit of elementary charge is shown as a function of the number of nearest-neighbor N atoms to a Si atom (see Table I).

TABLE I. The effective charge on N and Si atoms (Q^*_N and Q^*_{Si}) for each configuration in Fig. 3 and for Si_3N_4 crystals. The number of adjacent N atoms for a Si atom is denoted by Roman numerals.

case	N(1)	N(2)	N(3)	N(4)	Si(1)	Si(2)	Si(3)	Si(4)	Si(5)	Si(6)	Si(7)
(a)	−1.37	−1.36			0.78(II)	0.35(I)	0.30(I)	0.37(I)	0.31(I)		
(b)	−1.34	−1.34			0.84(II)	0.82(I)	0.46(I)	0.48(I)			
(c)	−1.35	−1.35	−1.43		0.86(II)	0.80(II)	0.87(II)	0.46(I)	0.47(I)		
(d)	−1.27	−1.28	−1.28	−1.28	1.33	0.48(I)	0.45(I)	0.41(I)	0.47(I)	0.44(I)	0.41(I)
α–, β– Si_3N_4			−1.20					1.60(IV)			

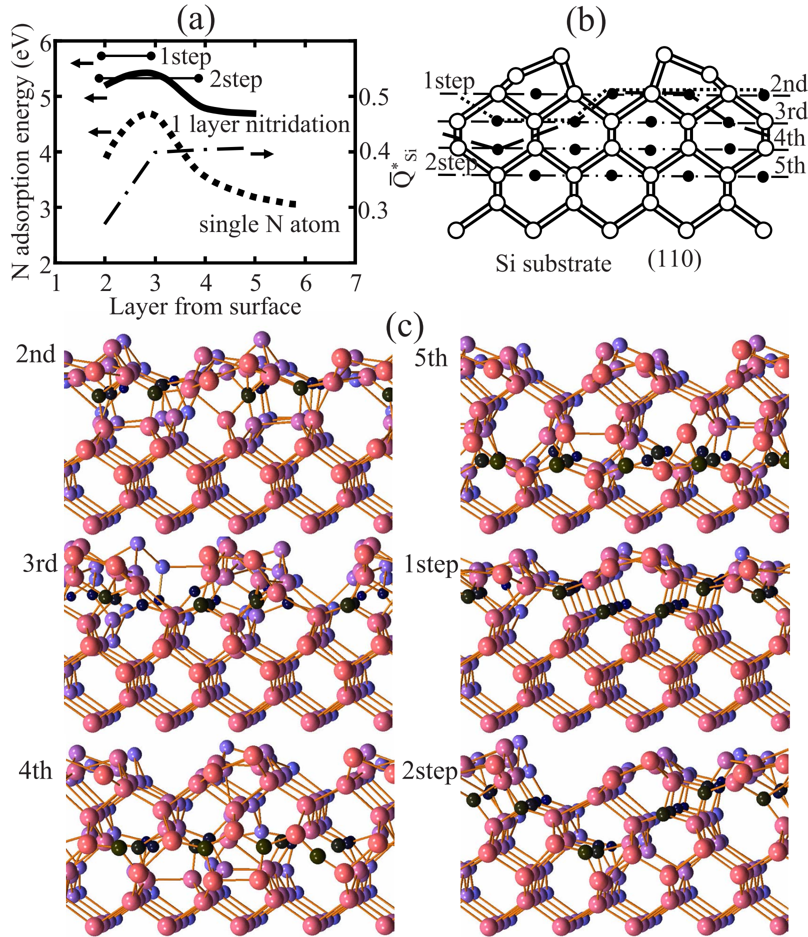

FIG. 4. (Color online) (a) Adsorption energy/N atom of a single N atom (broken line) and of one-layer nitridation (solid line), and of nitridation with steps ranging from second to third, and to fourth layers (ball-headed lines) as a function of depth from the Si(100) surface. The average effective charge on Si atoms adjacent to an N atom ($\bar{Q}^*_{\mathrm{Si}}$) with a unit of elementary charge is also shown as a function of the depth from the Si(100) surface. (b) Initial configurations for N split-interstitial atoms below the Si(100) surface. Dark circles represent N atoms and bright circles represent Si atoms. (c) N-condensed structures after relaxation for one monolayer on the second, third, fourth, and fifth layers, and 1-step structure and 2-step structure between the second and fourth layers. Dark balls represent N atoms. Bright balls represent Si atoms from red to blue according to the depth.

remains the same in Fig. 3(c) [N(1)-Si(1)-N(2), N(1)-Si(2)-N(2), and N(2)-Si(3)-N(3)], but is decreased in Fig. 3(d) compared to Fig. 3(b).

To understand the influences of the adjacent N atom on the Si-N bond strength in an N-Si-N bond, we calculated an effective charge of valence electrons on each atom. The effective charge Q^* (effective electronic+core charges), summed on N and Si atoms for each configuration in Fig. 3 and for Si_3N_4 crystals, are tabulated in Table I. Although the effective charge Q^*_{N} on each N atom slightly changes from -1.27 to -1.43, strong correlation between the effective charges on N atoms is not clear from Figs. 3(a)–3(d), and for Si_3N_4. This difference may have risen from the differences in atomic density and atomic conformation around N atoms among these structures. As for the effective charges on Si atoms ranging from 0.30 to 1.33, the influences of the increase in the nearest-neighbor N atoms are more evident. The average effective charge $\bar{Q}^*_{\mathrm{Si}}$ is shown as a function of the nearest-neighbor N atoms in Fig. 3(e); the case [Fig. 3(d)] is neglected here because both N and Si atoms are close to Si(1). Si atoms from Figs. 3(a)–3(d) are thus positively charged almost proportionally to the number of Si-N bonds. Here, the cohesive energy between a N and the nearest-neighbor Si atoms is simply estimated by the electrostatic energy (E_{es})$-\Sigma Q^*_X * Q^*_Y / r_b$ based on the effective charges, where Q^*_X, Q^*_Y, and r_b represent the effective charge on an X atom, the effective charge on a Y atom, and the X-Y atomic distance, respectively. The energy difference between $E(\mathrm{Si_{cry}})+E(\mathrm{N_{atoms}})$ and $E(\mathrm{Si_{cry}}$ with N) is also expressed as $-\Sigma Q^*_X * Q^*_Y / r_b$ by using the effective charge Q^* induced on N and Si atoms. $E(\mathrm{Si_{cry}})+E(\mathrm{N_{atoms}})$ is automatically evaluated as zero because of an induced charge Q^* of zero in each system. The E_{es} for a single N atom in crystalline Si shown in Fig. 2(a) is thus estimated to be 4.6 eV (3.05 eV by first-principles calculations). When this argument is applied to Si oxidation, the E_{es} for an O atom isolated in a Si-Si bond in crystalline Si is estimated to be 6.9 eV (5.0 eV by first-principles calculations). Cohesive energy in covalent materials may be overestimated because strain energy is neglected; but it reflects the general tendency in materials. The E_{es} enhancement in Si oxidation is not as remarkable as in Si ni-

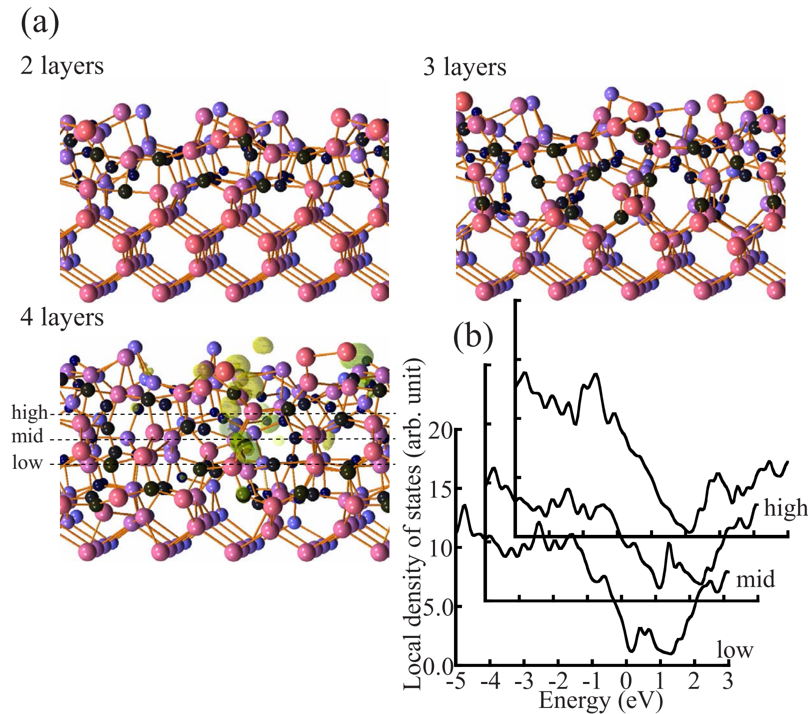

FIG. 5. (Color online) (a) two-, three-, and four-layer nitrided structures ranging from the second to third layers, from the second to fourth layers, and from the second to fifth layers when the ratio of numbers of Si and Ni atoms is 1:1. Dark balls represent N atoms. Bright balls represent Si atoms from red to blue according to the depth. Yellow isosurfaces represent the electronic charges of states between 0 and 1 eV. (b) LDOS at the low, mid, and high layers of Si nitride denoted by broken lines in (a).

tridation. The fact that E_{es} enhancement with number of N atoms is described reasonably by the effective charges suggests that E_{es} increases due to charge transfers from N atoms. The increase in E_{es} in proportion to the number of Si-N bonds is thought to have a strong influence on condensation of N atoms in crystalline Si observed in Fig. 1(b).

The cohesive energy of a finite SiN cluster is smaller than an infinite Si-N bond network. The difference can be understood by taking into account the Si-Si-N bond at the interfaces between the SiN cluster and the surrounding crystalline Si. The small number of the nearest N atoms adjacent to a Si atom at the interface suppresses the Si ionization, resulting in a weak ionic interaction between Si and N atoms. This is considered to be the reason that finite SiN clusters in a Si crystal show cohesive energies comparatively smaller than infinite Si-N bond networks. Consequently, once SiN clusters are agglomerated, they maintain a smaller interface size, resulting in a larger-scale agglomerated structure observed in Fig. 1(b).

D. N condensation in Si(100) substrate

Another important aspect of N adsorption in Si(100) substrates is that it has strong dependence on the depth from the surface as reported by Kim *et al.*[13] The calculated adsorption energy of an N atom at a stable split-interstitial configuration is shown as a function of the depth with a broken line in Fig. 4(a). As clearly seen, the split-interstitial site at the third layer is energetically the most stable, except for a surface dimer configuration.[9]

To understand this phenomenon, an effective charge on each atom was analyzed. As shown by a dash-dotted line in Fig. 4(a), the average effective charge on the Si atoms adjacent to the N atom $(\bar{Q}^*_{\mathrm{Si}})$ is reduced from 0.41 in a bulk Si slightly to 0.40 at the third layer, and dramatically to 0.26 at the second layer as the N atom approaches the surface because of the charge-transfer reduction from the Si atoms located closest to the surface. This results in smaller E_{es} between N and Si atoms near the surfaces. Thus, the N atom at the third layer is the most stable, where the strain energy gain and the E_{es} reduction between Si atom and N atom toward the surface are well balanced.

When N atoms are introduced almost simultaneously on the Si(100) surface, the simultaneous N incorporation may lead to a fast condensation of SiN clusters before stabilizing at the most stable site [the top of the broken line in Fig. 4(a)]. This will lead to nonuniformly agglomerated SiN film structures observed in Fig. 1(b). If N atoms are introduced slowly enough, however, they have a higher probability of arriving at the most stable third layer. It is due to a small migration energy of 0.5 eV and a large energy barrier of Si atom substitution by an N interstitial atom shown in Fig. 2. Then, the N atoms arriving at the third layer will form an N-Si-N cluster together to organize a Si-N network on the same layer, as the number of incorporated N atoms increases. Condensation of N atoms generates kinetic energies, forming Si-N bond networks at moderately high temperature, although simple Si atom substitution by an N atom may not be easy because of large energy barriers (Fig. 2). Since the global geometry optimization costs an enormous amount of time, we considered

plausible condensation models for one monolayer on a layer, and 1.25 layer for one- and two-step structures, between the second and fifth layers shown in Fig. 4(b). 16 or 20 N atoms are prepared at split-interstitial sites (the most stable interstitial configuration for N atoms in Fig. 2) on each layer, and 1- and 2-step structures, respectively. First, the atoms were moved with molecular dynamics, while reducing kinetic energies, and then were relaxed to realize the most stable configuration [Fig. 4(c)]. Adsorption energy of N atoms by Si-N condensation on the second, third, fourth, and fifth layers was calculated to be 5.18, 5.39, 4.75, and 4.72 eV/N atom, respectively [a solid line in Fig. 4(a)]. The adsorption energy for 1-step structure ranging from the second to third layers was as large as 5.77 eV/N atom. This is because N atoms are located at the second-nearest neighbors. The adsorption energy for 2-step structure ranging between the second and fourth layers was, however, reduced to 5.30 eV/N atom [ball-headed lines in Fig. 4(a)]. Although the adsorption energy for condensation slightly deviates along the depth direction, the adsorption energy around the third layer condensation is larger than those of agglomerated clusters shown in Fig. 3. It means that the nitridation around the third layer is the most plausible if the N incorporation is slow enough.

The energy gain by Si-N network organization along the depth direction is our next concern. We performed nitridation of two layers ranging from the second to third layers with 32 N atoms, three layers ranging from the second to fourth layers with 48 N atoms, and four layers ranging from the second to fifth layers with 64 N atoms, where the number is the same as the number of Si atoms shown in Fig. 5(a). N atoms were prepared initially at the split-interstitial sites shown in Fig. 4(b). The adsorption energy/N atom of the Si nitride layers increases in proportion to the layer thickness from 5.39 eV for one layer to 5.48 eV for two layers; furthermore to 5.64 eV for three layers, but it slightly decreases down to 5.50 eV for four layers, when the nitridation was simply extended from the most stable third layer. The adsorption energy/N atom will be summarized later in Fig. 7(c). Since N atoms become more stable by forming an alternate Si-N-Si-N bond order rather than a nonalternate N-Si-Si-N bond order, incorporated N atoms will be adsorbed at the interfaces between crystalline Si and a SiN cluster layer once the flat SiN cluster layer was formed. This scenario will lead to a SiN growth mode with a flatter and more uniform interface without deteriorating into agglomeration, and this is what was experimentally observed with a slow growth mode at a moderately high temperature [Fig. 1(c)].

Local density of states (LDOS) around the low, mid, and high layers denoted by three broken lines in the Si nitride for four layers nitridation in Fig. 5(a) were calculated as shown in Fig. 5(b). The band gaps for these layers in the Si nitride are not fully opened, indicating that the coordination of Si-N bonds is not good enough. Furthermore, DBs exist obviously around the gap even in the mid layer of Si nitride, as evidenced by the yellow isosurfaces in the Si nitride for four-layer nitridation [Fig. 5(a)]. The yellow isosurfaces represent the electronic charges of states between 0 and 1 eV. The generated Si nitride becomes more stable with growing film thickness of up to three layers because of almost periodic Si-N-Si-N bond formation along the depth direction. The adsorption energy/N atom is, however, reduced as the Si nitride thickness exceeds three layers [the broken line in Fig. 7(c)]. It reveals that the internal local strain has accumulated increasingly in the Si nitride. The average energy gain by the N atoms at the fourth layer was estimated to be as small as 5.0 eV. The reduction of adsorption energy with Si nitride thickness suggests that further nitridation may become more difficult, even if further interstitial N atoms migrate to the interface. This corresponds to the experimentally observed fact that the Si nitridation is limited to a few nanometers in thickness.

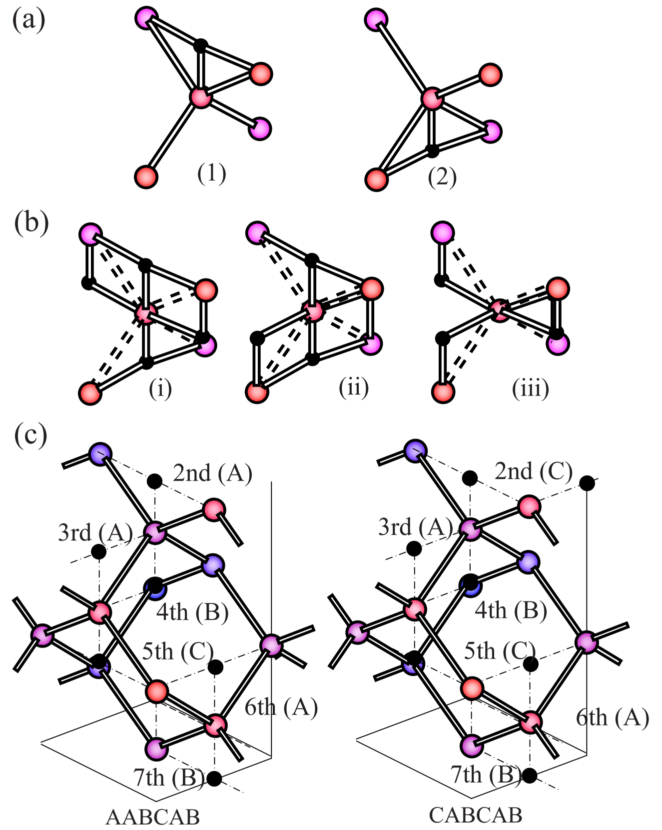

FIG. 6. (Color online) (a) N split-interstitial configuration units (1) and (2) for threefold coordination with Si atoms. (b) Configuration units (i), (ii), and (iii) for Si atoms at fourfold coordination with N atoms. (c) Construction of AABCAB and CABCAB with units structure A, B, C. Dark circles represent N atoms. Bright circles represent Si atoms from red to blue according to the depth.

E. Uniformly grown Si nitride on Si(100)

Since a uniform Si nitride can be formed on Si(100) with appropriate experimental procedures, we need to understand the most stable and realistic structure of Si nitrides on Si(100). To the best of the authors' knowledge, α-Si_3N_4, β-Si_3N_4, or other types of crystalline Si nitrides[20] cannot be formed on a Si(100) substrate. Another type of structure must have grown as a Si nitride on the Si(100) substrate. Furthermore, Si nitrides generated in Si(100) substrates are almost free from DBs.[21,22]. Since chemisorption of one threefold coordinated N atom, however, inevitably generates a DB in a bulk Si, some kinds of periodicity may exist in Si-N

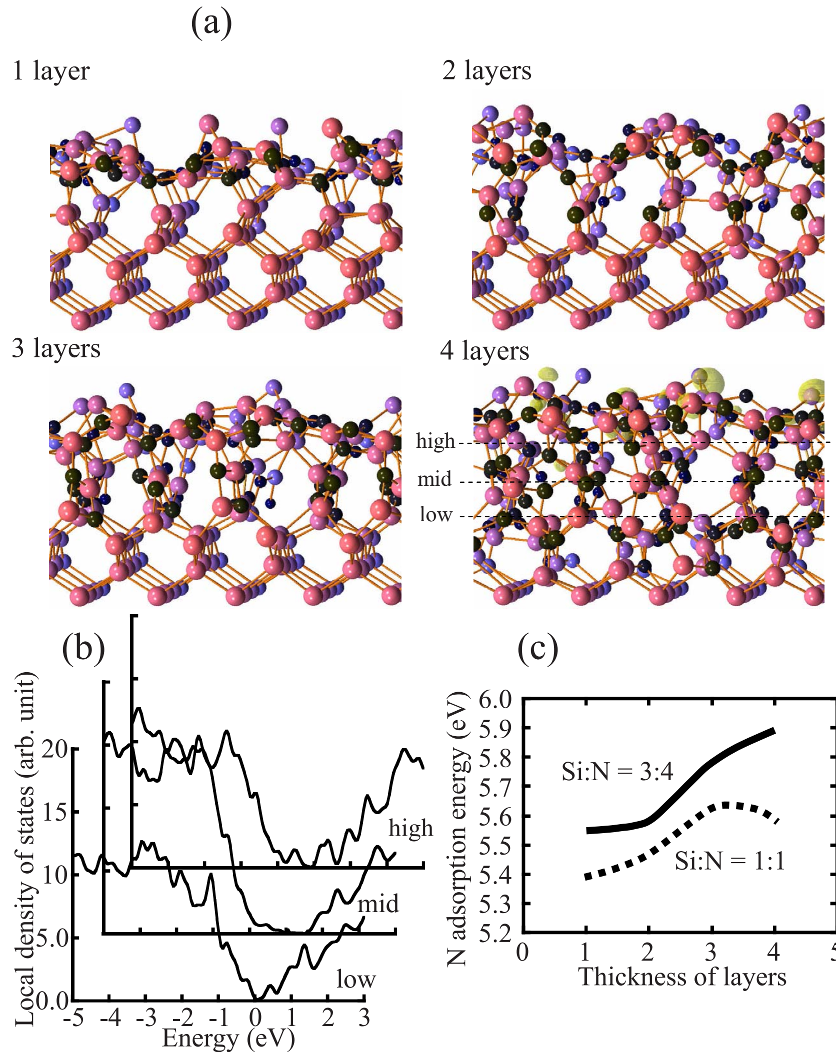

FIG. 7. (Color online) (a) one-, two-, three-, and four-layer nitrided structures ranging on the second layer, from the second to third layers, from the second to fourth layers, and from the second to fifth layers when the ratio of number of Si and Ni atoms is 3:4. Dark balls represent N atoms. Bright balls represent Si atoms from red to blue according to the depth. Yellow isosurfaces represent the electronic charges of states between 0 to 1 eV. (b) LDOS at the low, mid, and high layers of Si nitride denoted by broken lines in (a). (c) Adsorption energy/N atom of one-, two-, three-, and four-layer nitridation as a function of depth from the Si(100), when the ratio of numbers of Si and N atoms is 1:1 and 3:4.

network organization in the Si nitride on Si(100) to eliminate DBs. Although structures for monolayer Si nitride have been proposed,[14,23,24] knowledge of thick Si nitrides on Si(100) is lacking. Hence, we consider plausible model structures for a uniform Si nitride without defects on Si(100) substrates. Since N atoms in a Si nitride are normally threefold coordinated and Si atoms in the Si nitride are fourfold coordinated, Si-N bond network organization without DBs may not be easy. We try to consider Si-N bond organization without generating defects on each layer in a Si(100) substrate. The initial N-atom configurations prepared for this structure can be strictly limited by assuming a periodic Si nitride structure toward the Si(100) depth direction. In the case of Si oxidation, it proceeds as O atom incorporation into stable Si-Si bonds in the vicinity of SiO_2/Si interfaces. This is clearly evidenced by the residual order specific to O atom incorporation.[25]

Since the N atom at a split-interstitial site is the most stable in crystalline Si, we employed two types of N split-interstitial configurations with threefold coordination for constructing a periodic structure in the Si crystal shown in Fig. 6(a). The N atom is in a split-interstitial site with (1) a lower Si atom or (2) a higher Si atom. Although there are other types of split-interstitial configurations along a hexagon in the crystal Si, those structures may be identical in terms of symmetry operations. On the other hand, by employing the two units as structural environments for a Si atom, three types of Si configurations in fourfold coordination with adjacent N atoms can be constructed as shown in Fig. 6(b). Si atoms can be fourfold coordinated with N atoms in (i) a plane normal to the surface, (ii) a plane normal to the surface with 90° rotation, and (iii) a plane parallel to the surface. Based on these configurations, we can conceive three types of Si nitride layers; A, B, C in Si(100) substrates.

A: N atoms are bonding with the lower Si atoms, as shown in (1) of Fig. 6(a). The number of N and Si atoms is the same. B: N atoms are bonding with the higher Si atoms as shown in (2) of Fig. 6(a). The number of N and Si atoms is the same. C: A half of N atoms are bonding with the higher Si atoms, and the latter half is bonding with the lower Si atoms shown in (1) and (2) of Fig. 6(a). The number of N atoms is twice that of Si atoms. These layer structures are stacked repeatedly as *ABCABC*... from the surface toward the depth direction. By following this scheme, the ratio of numbers of Si and N atoms must be 3:4, and the DBs are fully eliminated in crystalline Si. When we start nitridation from the second layer in a Si(100) substrate, there are several possible Si nitride organization orders of *CABCABC*... and *AABCABC*... [Fig. 6(c)], or *ABCABCA*... and *BCABCAB*..., where the second layer is boundary conditioned with C-, A-, or B-type layer. The arrangement of DBs and their number on the second layer depends on these boundary conditions.

As a typical example, the layered structure of C, CA, CAB, and CABC layers with C top layer, which has fewer DB, was prepared. Since Si atoms are initially coordinated with N atoms in planar arrangement, the Si-N bonds are mutually in unfavorable orientations, and the Si nitride structures are not so stable. After the atoms were initially prepared, they were moved and relaxed to realize the most stable configuration following the method described in Sec. III D. Although the relaxation generates kinetic energy, unfavorably spurious bonds such as N-N bonds are rarely formed. The final structures are shown in Fig. 7(a). The translational symmetry of a bulk Si seems to remain for thinner Si nitride. The adsorption energy/N atom in the nitride layers further increases in proportion to the layer thickness from 5.55 to 5.58 eV for one and two layers, respectively; furthermore, to 5.78 eV for three layers, and still increases further to 5.90 eV for four layers because of relatively lower strain. These adsorption energies represented by a solid line in Fig. 7(c) are definitely higher in a thick region and are not saturated yet compared with the broken line in the case of N and Si atoms with the same number. The stable Si nitride can be formed on Si(100) with the N adsorption energy difference of 1 eV from those of the crystalline Si nitride.[18] This is mostly due to the forming of a fully periodic Si-N bond structure. The energy difference is ascribable to unfavorable Si-N bond orientations.

LDOS at the low, mid, and high layers denoted by three broken lines in the Si nitride for four-layer nitridation in Fig. 7(a) were calculated as shown in Fig. 7(b). The band gap opens widely especially in the midlayer of Si nitride, although the density of DB states in the gap is low, suggesting that the structure is more stable than in the case in Fig. 5(b). DBs have almost disappeared in the midlayer, as evidenced by few yellow isosurfaces in the Si nitride for four-layer nitridation [Fig. 7(a)]. The yellow isosurfaces represent the electronic charges of states between 0 and 1 eV. This may be the ideal structure for uniformly grown Si nitrides on Si(100) and moreover, the structure may be experimentally obtainable. Since the number of DBs in Si nitrides generated in Si(100) substrates has been reduced,[21,22] Si nitride grown on Si(100) will become closer to the ideal structure with a well-controlled growth rate from those described in Sec. III D.

IV. CONCLUSION

In conclusion, we performed Si(100) nitridation, which was found to be strongly dependent on temperature and growth rates by AFM measurements. Then, we analyzed Si nitridation mechanisms based on first-principles calculations. Rapid N incorporation into crystalline Si brings about agglomeration of an Si_3N_4 material because of E_{es} enhancement induced by charge transfers between Si and N atoms, but gradual N incorporation on Si(100) seems to form a thin Si nitride layer around the third layer, and then it grows more as an atomically flat and highly coordinated Si nitride. The continuation of nitridation normally leads to reduction of N adsorption energy and will be limited with certain Si nitride thickness because of increasing strain energy. However, the stable and ideal structures of uniform and thick Si nitrides with a small number of defects on Si(100) are predicted to grow more.

ACKNOWLEDGMENTS

The authors would like to thank M. Takayanagi, K. Eguchi, and T. Yamasaki for their support.

*kato@arl.rdc.toshiba.co.jp

[1] J. W. Kim and H. W. Yeom, Surf. Sci. **546**, L820 (2003).
[2] A. Nakajima, Q. D. M. Khosru, T. Yoshimoto, T. Kidera, and S. Yokoyama, Appl. Phys. Lett. **80**, 1252 (2002).
[3] K. T. Queeney, Y. J. Chabal, and K. Raghavachari, Phys. Rev. Lett. **86**, 1046 (2001).
[4] Y. K. Kim, H. S. Lee, H. W. Yeom, D.-Y. Ryoo, S.-B. Huh, and J.-G. Lee, Phys. Rev. B **70**, 165320 (2004).
[5] D. Matsushita, H. Ikeda, A. Sakai, S. Zaima, and Y. Yasuda, Jpn. J. Appl. Phys., Part 1 **40**, 2827 (2001).
[6] H. Watanabe, K. Kato, T. Uda, K. Fujita, M. Ichikawa, T. Kawamura, and K. Terakura, Phys. Rev. Lett. **80**, 345 (1998).
[7] K. Kato, T. Uda, and K. Terakura, Phys. Rev. Lett. **80**, 2000 (1998); K. Kato and T. Uda, Phys. Rev. B **62**, 15978 (2000).
[8] T. Yamasaki, K. Kato, and T. Uda, Phys. Rev. Lett. **91**, 146102 (2003); K. Kato, T. Yamasaki, and T. Uda, Phys. Rev. B **73**, 073302 (2006).
[9] H.-J. Kim and J.-H. Cho, Phys. Rev. B **69**, 233402 (2004).
[10] K. Kato, Y. Nakasaki, and T. Uda, Phys. Rev. B **66**, 075308 (2002).
[11] D. Vanderbilt, Phys. Rev. B **41**, 7892 (1990).
[12] E. Wigner and F. Seitz, Phys. Rev. **43**, 804 (1933).
[13] J. W. Kim, H. W. Yeom, K. J. Kong, B. D. Yu, D. Y. Ahn, Y. D. Chung, C. N. Whang, H. Yi, Y. H. Ha, and D. W. Moon, Phys. Rev. Lett. **90**, 106101 (2003).
[14] G.-M. Rignanese and A. Pasquarello, Appl. Phys. Lett. **76**, 553

(2000).
[15] P. A. Schultz and J. S. Nelson, Appl. Phys. Lett. **78**, 736 (2001).
[16] H. Sawada and K. Kawakami, Phys. Rev. B **62**, 1851 (2000).
[17] H. Kageshima and A. Taguchi, Appl. Phys. Lett. **76**, 3718 (2000).
[18] Y.-N. Xu and W. Y. Ching, Phys. Rev. B **51**, 17379 (1995).
[19] P. A. G. O'Hare, I. Tomaszkiewicz, and H. J. Seifert, J. Mater. Res. **12**, 3203 (1997).
[20] A. Zerr, G. Miehe, G. Serghiou, M. Schwarz, E. Kroke, R. Riedel, H. Fues, P. Kroll, and R. Boehler, Nature (London) **400**, 340 (1999).
[21] K. Kato, Y. Nakasaki, D. Matsushita, and K. Muraoka, Proceedings of the ICPS-27, 2005 (unpublished), p. 395; K. Kato, D. Matsushita, K. Muraoka, and Y. Nakasaki, Proceedings of ICPS-28, 2007 (unpublished), p. 1403.
[22] D. Matsushita, K. Muraoka, K. Kato, Y. Nakasaki, S. Inumiya, K. Eguchi, and M. Takayanagi, Tech. Dig. - Int. Electron Devices Meet. **2005**, 847; D. Matsushita, K. Muraoka, Y. Nakasaki, and K. Kato, Tech. Dig. VLSI Symp. 2004, 172.
[23] J. H. G. Owen, D. R. Bowler, S. Kusano, and K. Miki, Phys. Rev. B **72**, 113304 (2005).
[24] Y. Morita, T. Ishida, and H. Tokumoto, Jpn. J. Appl. Phys., Part 1 **41**, 2459 (2002).
[25] K. Tatsumura, T. Shimura, E. Mishima, K. Kawamura, D. Yamasaki, H. Yamamoto, T. Watanabe, M. Umeno, and I. Ohdomari, Phys. Rev. B **72**, 045205 (2005).